Fiber-laser-based, high-repetition-rate, picosecond ultraviolet source tunable across 329-348 nm

KAVITA DEVI,[1,*] S. CHAITANYA KUMAR,[1] AND M. EBRAHIM-ZADEH[1,2]

[1]*ICFO-Institut de Ciencies Fotoniques, The Barcelona Institute of Science and Technology, 08860 Castelldefels (Barcelona), Spain*
[2]*ICREA, Passeig Lluis Companys 23, 08010 Barcelona, Spain*
**Corresponding author: kavita.devi@icfo.es*

Received XX Month XXXX; revised XX Month, XXXX; accepted XX Month XXXX; posted XX Month XXXX (Doc. ID XXXXX); published XX Month XXXX

We report a compact, fiber-laser-based, high-repetition-rate picosecond source for the ultraviolet (UV), providing multi-tens of milliwatt of average power across 329-348 nm. The source is based on internal sum-frequency-generation (SFG) in a singly-resonant optical parametric oscillator (OPO), synchronously pumped at 532 nm by the second harmonic of a picosecond Yb-fiber laser at 80 MHz repetition rate. Using a 30-mm-long single-grating MgO:sPPLT crystal for the OPO and a 5-mm-long BiB_3O_6 crystal for intracavity SFG, we have generated up to 115 mW of average UV power at 339.9 nm, with >50 mW over 73% of the tuning range for 1.6 W of input pump power. The UV output exhibits passive rms power stability of ~2.9% rms over 1 min and 6.5% rms over 2 hours, in high beam quality. Angular acceptance bandwidth and cavity length detuning with pump power and crystal temperature have also been studied. © 2016 Optical Society of America

OCIS codes: *(190.4970) Parametric oscillators and amplifiers; (190.4360) Nonlinear optics, devices; (190.4400) Nonlinear optics, materials; (190.2620) Harmonic generation and mixing; (140.3610) Lasers, ultraviolet.*

http://dx.doi.org/10.1364/OL.99.099999

Tunable ultrafast UV laser sources are of great interest for many industrial and medical applications including laser micromachining [1], optical data storage [2], combustion diagnostics, atmospheric sensing and bio-imaging [3]. For many years, the most effective approach to development of ultrafast UV sources has been based on nonlinear conversions, namely frequency tripling and quadrupling of mode-locked lasers, including Kerr-lens-mode-locked (KLM) Ti:sapphire laser, Nd:YAG laser, mode-locked EDFA, and more recently Yb-fiber lasers [4-6]. Although, such ultrafast sources are capable of providing high average power, with the exception of the KLM Ti:sapphire laser [7], such techniques result in fixed UV wavelengths. On the other hand, synchronously-pumped optical parametric oscillators (OPOs) are viable ultrafast sources of tunable coherent radiation, providing high average powers across broad spectral regions in the near- and mid-infrared (IR) [8]. To expand the spectral coverage of OPOs to shorter wavelengths, intracavity frequency doubling or sum-frequency-generation (SFG) has been previously demonstrated in various time-scales from continuous-wave (cw) to femtosecond domain [9-12]. With the advent of quasi-phase-matched nonlinear materials such as MgO:sPPLT with high photorefractive damage threshold, high-average-power picosecond OPOs synchronously pumped in the green are also now well-established [13]. Recently, using internal frequency doubling of the resonant signal in such an OPO, tunable picosecond output generation in the UV was demonstrated [14]. While this approach was shown to provide significant tunability in the UV across 317-340 nm, the output power was relatively low, and a drop in the UV power was observed after short-term operation. Further, material dispersion necessitated the use of multiple grating periods in the MgO:sPPLT crystal to achieve extended signal coverage in the visible (634-681 nm) so as to enable the tunability in the UV. On the other hand, intracavity SFG of near-IR signal and green pump radiation in such an OPO could result in tunable UV generation, while operating near degeneracy, where widely tunable near-IR signal radiation using a single grating period in MgO:sPPLT is attainable, with the additional advantage of low oscillation threshold. We have earlier demonstrated this technique in a green-pumped cw OPO, generating tunable UV output [15]. Here we demonstrate that it is possible to exploit this approach in picosecond time-scale, for the generation of practical-average-power pulses at high repetition rate with significant tuning in the UV. The described source provides multi-tens of milliwatt of average power across 329-348 nm under long-term operation, while using single grating period in MgO:sPPLT. We have generated as much as 115 mW of output power at 339.9 nm, and >50 mW across 73% of UV tuning range for a pump power of 1.6 W at 80 MHz, with good passive power stability and beam quality, and without any power degradation or damage to the nonlinear crystal in long-term operation. To the best of our knowledge, these are the highest average powers generated at such high repetition rates in the picosecond time-scale with tunability in this UV spectral range.

The schematic of the experimental setup for the tunable picosecond source is shown in Fig. 1. The fundamental pump source is a mode-locked Yb-fiber laser delivering up to 20 W of average power at 1064 nm in pulses of 20 ps duration at 80 MHz repetition rate. The green pump radiation for the OPO is obtained by external single-pass second-harmonic-generation (SHG) of the laser in a 30-mm-long LiB_3O_5 (LBO) crystal cut at θ=90° (φ=0°) for type I ($oo \rightarrow e$) noncritical interaction [5]. To maintain stable output characteristics, the Yb-fiber laser is operated

at maximum power and a combination of a half-wave plate, HWP (H_1), and a polarizing beam-splitter (PBS_1) is used for power attenuation. A second HWP, H_2, is used to adjust the pump polarization for phase-matching in LBO. The SHG stage provides as much as 9.1 W of average power at 532 nm in pulses of 16.2 ps duration for a fundamental power of 16.8 W in a circular (>97%) beam with TEM_{00} mode profile [5]. To pump the OPO, the green pump source is operated at maxmium power, with the output beam collimated using lens, L_2, and a second pair of a HWP (H_3) and PBS_2 used for power attenuation. An additional HWP, H_4, is used to adjust the pump polarization for phase-matching in the OPO crystal, which is a 30-mm-long, 2.14-mm-wide, and 1-mm-thick, 1% bulk MgO:sPPLT. The crystal is housed in an oven with a stability of ± 0.1 ºC, enabling temperature tuning from 25 ºC to 200 ºC. The crystal contains a single grating period (Λ = 7.97 μm), and its end-faces are antireflection (AR)-coated (R <1%) over 800–1100 nm. The AR coating has a residual reflectivity of 1% to 15% for the idler over 1100–1400 nm. For intracavity SFG, we use a 5-mm-long BiB_3O_6 (BIBO) crystal with an 8x4 mm^2 aperture, cut at θ=136º (φ=90º) for type I ($ee \rightarrow o$) interaction, and AR-coated for 532 nm, 850-970 nm, and 325-350 nm. The OPO is configured in a folded ring cavity comprising four concave mirrors, $M_{1,2}$ (r=-100 mm), $M_{3,4}$ (r=-50 mm), and two plane mirrors, $M_{5,6}$. Mirror, M_1, is highly reflecting for the signal (R>99% over 840-1000 nm), and transmitting for the pump

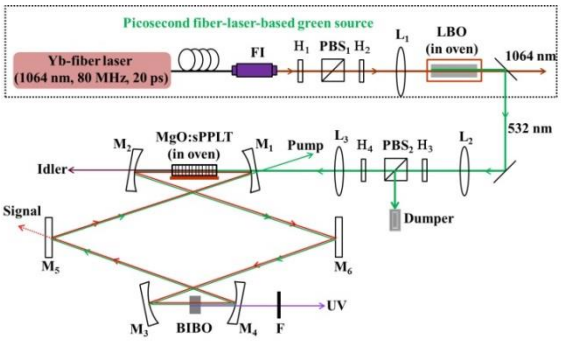

Fig. 1. Schematic of the experimental setup. FI: Faraday isolator, H_{1-4}: half-wave plate, $PBS_{1,2}$: polarizing beam-splitter; L_{1-3}: lens; M_{1-6}: mirror, F: filter.

(T>95% at 532 nm) and idler (T>85% over 1100-1500 nm). Mirrors, M_{2-6}, are highly reflecting for the signal (R>99% over 877-985 nm) and the pump (R>97% at 532 nm), while transmitting for the idler (T>80% over 1100-1400 nm) and the UV (T>80% over 310-390 nm). Thus, the OPO cavity ensures singly-resonant oscillation for the signal with a single-pass pump. A lens, L_3, of focal length, f = 250 mm, is used to focus the pump beam at the center of the MgO:sPPLT crystal, to a waist radius of w_{p1}~30 μm, while the design of the OPO resonator results in a primary signal waist radius of w_{s1}~41 μm at the center of the MgO:sPPLT crystal, and secondary pump and signal waist radii of w_{p2}~13 μm and w_{s2}~17 μm, respectively, at the center of the BIBO crystal, between mirrors M_3 and M_4. The total optical length of the OPO cavity is ~1.25 m, corresponding to a repetition rate of 240 MHz for the signal, which results in a compact cavity, and optimum mode-matching for SFG in the BIBO crystal. Given the green pump repetition rate of 80 MHz, the UV output is also at 80 MHz.

In order to characterise the OPO, we initially performed power scaling measurements of the idler and the corresponding leaked-out signal, without the intracavity BIBO, and with the MgO:sPPLT crystal at 100 ºC. As shown in Fig. 2, the idler and signal power increase linearly up to the maximum pump power. We extracted as much as 603 mW of idler at 1224 nm, together with 111 mW of signal at 941 nm, for pump power of 2 W. The OPO threshold is as low as 85 mW, with an idler extraction efficiency of ~30%. The high spatial quality of the green pump beam together with the advantage of near-degenerate operation in this work resulted in the low pump power threshold for the OPO. We then inserted the BIBO crystal into the cavity and simultaneously measured the repetition rate of the output signal pulses at 941 nm, using an InGaAs photo-detector (20 GHz, 18.5 ps) and a fast oscilloscope (3.5GHz, 40GS/s). The result is shown in the inset of Fig. 2, where a repetition rate of 240 MHz for the signal, synchronized to the third harmonic of the pump laser repetition frequency of 80 MHz is confirmed. The large amplitude of the first harmonic in the signal pulse train relative to the second- and third-harmonic peaks is due to the high responsivity of the photodetector in the near-IR, resulting in the detection of the idler at 1224 nm as well as the signal at 941 nm.

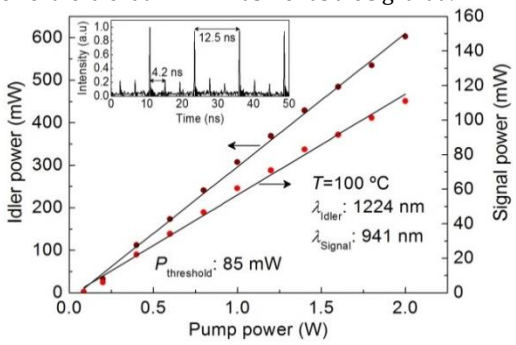

Fig. 2. Idler and leaked-out signal power scaling without the intracavity BIBO. Inset: Signal pulse train at 240 MHz (4.2 ns).

To characterize the intracavity SFG for UV generation, we measured the UV average output power as a function of pump power to the OPO, keeping the MgO:sPPLT crystal temperature fixed at 100 ºC. We adjusted the angle of the BIBO crystal for phase-matched SFG between the green pump and the corresponding signal to generate UV at 339.9 nm, at low pump power. Figure 3 shows the power scaling results for the UV. For a maximum input pump power of 2.2 W, we were able to generate as much as 115 mW of UV power. The threshold of the OPO with intracavity SFG was 98 mW. While measuring the UV output, the OPO cavity length was always optimized for maximum UV power generation, as the cavity detuning can vary the signal and green pump

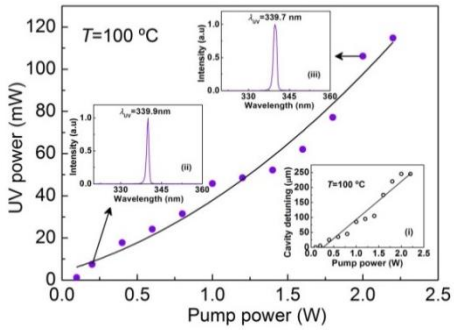

Fig. 3. UV power as a function of pump power to the OPO. Inset: (i) Variation of OPO cavity length as a function of pump power, and UV spectrum at (ii) low, and (iii) high pump power.

ratio for a given fixed phase-matched angle. The inset (i) of Fig. 3 shows the cavity detuning for optimum UV generation as a function of pump power, confirming positive cavity length detuning with the increase in pump power. In order to verify the effect of cavity detuning on the generated UV wavelength, we recorded the spectrum of the UV output using a spectrometer with resolution of 0.2 nm at low and high pump power, as shown in inset (ii) and (iii) of Fig. 3, respectively. At a pump power of 200 mW, the UV wavelength was recorded to be 339.9 nm,

while at 2 W of pump power it was 339.7 nm. Thus, the generated UV wavelengths at maximum power have a small blue shift of ~0.2 nm, as compared to lower pump powers. We also performed power scaling measurements for the corresponding idler and the leaked-out signal simultaneously under optimum UV power generation, as shown in Fig. 4. The idler and the signal power increase linearly up to a pump power of 1.6 W, beyond which a roll-off in the output powers is observed. The drop in the output power at higher pump powers could be attributed to the change in the cavity length, performed for maximum UV generation at each pump power level, as the power scaling results in Fig. 2, in the absence of intracavity BIBO, show no roll-off. To further confirm the cavity detuning effect, using the measured output signal power for a pump power of 2 W, and signal transmission of mirror M_5 at 941 nm, we have calculated the number of intracavity signal photons without and with the BIBO crystal to be 1.0518×10^{20} and 0.4169×10^{20} photons/sec, respectively. The corresponding number of generated UV photons at 339.9 nm is 0.001814×10^{20} photons/sec. A large decrease in signal photon number in the presence of BIBO crystal, as compared to that in the absence of the intracavity BIBO for the generation of 106 mW (0.001814×10^{20} photons/sec) of UV power implies that the number of intracavity signal photons was reduced by cavity detuning, which also resulted in lower pump depletion, and thus increased number of green photons for efficient SFG.

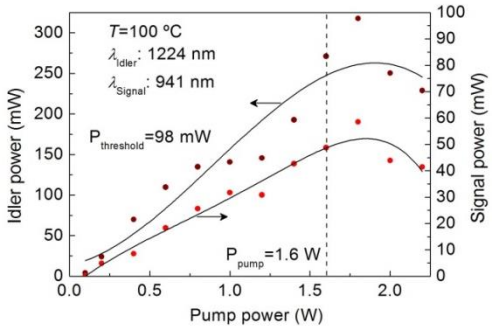

Fig. 4. Simultaneous power scaling for the idler and leaked-out signal under optimum intracavity SFG in BIBO.

The signal (at 941 nm) and the green pump beam, being *extraordinary*, experience a spatial walk-off angle of 69.5 mrad and 72.7 mrad in BIBO, respectively. Hence, under the present tight focussing condition, the effective interaction length in the crystal for SFG is limited to 0.317 mm. By optimizing the beam waists in BIBO using suitable mirrors, $M_{3,4}$, with larger radius of curvature, the interaction length in BIBO could be increased, resulting in higher UV power. Further, the spectral acceptance bandwidth of BIBO for SFG at 339.9 nm is calculated to be ~0.5 nm using relevant Sellmeier equations [16]. This is smaller than the broad double-peak signal spectrum (~10 nm) in green-pumped near-IR OPOs at high powers [13], due to self-phase-modulation of the signal pulses. Hence, by deploying dispersion compensation in the OPO cavity, or by using bandwidth reduction techniques such as use of diffraction grating and birefringent filter, spectral narrowing of the signal pulses could be achieved, thus further enhancing the generated UV power. The temporal walk-off between the signal and the green pump pulse in BIBO is calculated to be close to ~300 fs/mm across the signal tuning range, which results in a much longer temporal walk-off limited interaction length of ~54 mm as compared to the physical length of the crystal, thus confirming the negligible contribution of group velocity mismatch in SFG interaction.

Given the absence of output coupling for signal, there is a significant rise in the intracavity signal power with the increase in pump power. Therefore, to avoid thermal loading in MgO:sPPLT or any possible damage to the crystal at high pump powers, we limited the maximum pump power to 1.6 W, and characterized the device for spectral tuning. Using the single grating period, and varying the temperature of the crystal from 50 ºC to 200 ºC, we were able to tune the intracavity signal over 142 nm, across 866-1008 nm, with a corresponding idler tuning of 253 nm, over 1126-1379 nm. Thus, by simultaneously varying the phase-matching angle, θ, of intracavity BIBO over 137.6º-144º, UV spectral tuning across 329-348 nm could be achieved. Figure 5(a) and 5(b) show the average UV and the idler output power across the tuning range for an input pump power of 1.6 W. As evident, the SFG output is continuously tunable over the entire tuning range, providing >50 mW of UV power over 73% of the SFG tuning range, with a maximum of 87 mW at 332.3 nm. The drop in the UV power at longer SFG wavelengths is attributed to the drop in the reflectivity of mirrors, $M_{2\text{-}6}$, at longer signal wavelengths near degeneracy. The device can deliver >160 mW of near-IR power over 96% of the idler tuning range, with a maximum of 346 mW at 1199 nm, as can be seen in Fig. 5(b). For the generation of tunable UV, while changing the temperature of the MgO:sPPLT crystal and simultaneously varying the phase-matching angle in the BIBO crystal, we have also optimized the cavity length at each crystal temperature and phase matching angle for optimum UV power generation. Figure 5(c) shows the cavity detuning as a function of

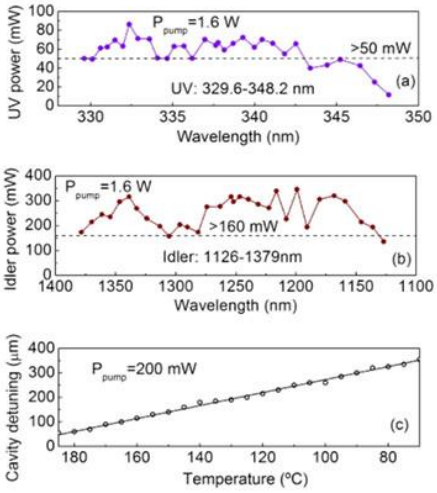

Fig. 5. (a) UV and (b) Idler power across the tuning range, at pump power of 1.6 W. (c) Cavity-length detuning versus crystal temperature.

MgO:sPPLT crystal temperature, at low pump power of 200 mW. It can be seen that as the crystal temperature decreases from 185 ºC to 70 ºC, the cavity length undergoes positive detuning, increasing by 300 μm, as the OPO operation moves towards degeneracy. The operation of the OPO above 185 ºC and below 70 ºC was not possible at 200 mW of pump power, as the OPO threshold away from degeneracy and close to degeneracy increased to >200mW, due to the reduction in parametric gain and the drop in the reflectivity of mirrors, respectively.

We also studied the angular tolerance for phase-matching in BIBO for UV generation by measuring the angular acceptance bandwidth at a pump power of 200 mW, with MgO:sPPLT crystal temperature fixed at 100 ºC. The variation of the normalized UV power at 339.9 nm as a function of internal angular deviation about the phase-matching angle for the 5-mm-long BIBO crystal is shown in Fig. 6. As evident, an experimental FWHM angular acceptance bandwidth of 0.45º is obtained, which is significantly wider than the theoretically calculated value of 0.025º, shown in inset (i) of Fig. 6. The deviation of the experimentally measured value from the theoretical calculation is attributed to the spatial walk-off in BIBO, which results in the decrease in effective interaction length, as also observed for β-BaB_2O_4 crystal in

earlier reports [6]. Using the spatial walk-off-limited effective length of 0.317 mm, we theoretically calculated the normalized UV power as a function of internal angular deviation, and obtained a FWHM angular acceptance bandwidth of 0.4°, as shown in the inset (ii) of Fig. 6, which is in close agreement with the experimentally measured value.

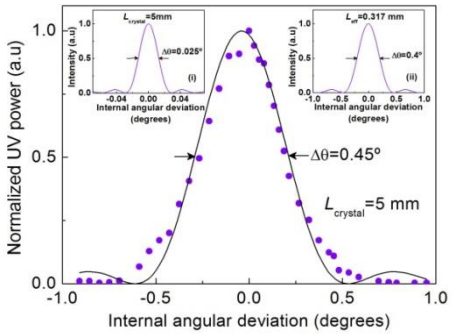

Fig. 6. Experimentally measured angular acceptance bandwidth for SFG at 339.9 nm in a 5-mm-long BIBO crystal. Inset: Theoretically calculated angular acceptance bandwidth for (i) 5-mm-long crystal and (ii) an effective length of 0.317 mm.

We further studied the output power stability of the UV source by performing measurements of short-term and long-term average power fluctuation. We recorded the passive power stability of the generated UV at 339.9 nm at a pump power of 1.5 W, and under free-running conditions. Figures 7(a) and 7(b) show the resulting short-term and long-term average power fluctuations, where the UV power is recorded to exhibit a passive rms stability better than 2.9% and 6.5% over 1 minute and 2 hours, respectively. The instability in power is attributed to the mechanical vibrations and air currents in the laboratory in the absence of active stabilization and thermal isolation of the cavity. At 1.5 W of pump power, the intracavity signal peak intensity at the centre of the BIBO crystal is ~200MW/cm^2. We have

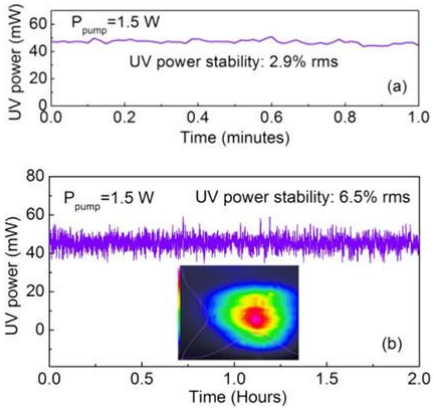

Fig. 7. Power stability of the generated UV over (a) short-term, and (b) long-term operation. Inset: Spatial beam profile of the circularized UV beam together with the intensity profiles measured in the far-field.

not observed any damage to the BIBO after long-term operation over many hours at these focused intensities. We also recorded the spatial profile of the UV output beam at 339.9 nm for a pump power of 1.6 W. Measured at a distance of 25 cm from the SFG crystal, the generated UV beam was elliptic with a circularity of ~40%, due to the spatial walk-off in BIBO. However, by placing a plano-convex lens of focal length f=100 mm after mirror M_4, we were able to significantly improve the circularity of the beam over a distance of 1 m from the BIBO crystal. The resulting far-field energy distribution of the UV beam, together with the orthogonal intensity profiles, are shown in the inset of Fig. 7(b), confirming a circularity of >75%. Over the entire tuning range, and even after long-term operation, we have not observed any degradation in the UV output beam quality.

In conclusion, we have demonstrated a compact tunable picosecond UV source, providing multi-tens of mW of output power across 329-348 nm at 80 MHz pulse repetition rate. The source is based on intracavity SFG between the input green pump and resonant signal radiation in an Yb-fiber-based picosecond OPO, and provides up to 115 mW of average UV power at 339.9 nm, with >50 mW over 73% of the tuning range. As compared to earlier work [14], the enhancement in the UV power has been achieved by control of cavity detuning effects, combined with high pump beam spatial quality and low OPO threshold power in near-degenerate operation. We believe these are the highest average powers generated with tunability in this UV spectral range in picosecond time scale at such high repetition rate. In addition to the UV, the device also provides tuning coverage across 1126-1379 nm with up to 346 mW of average power in the idler. The UV tuning range can be further extended to shorter wavelengths by using the same crystal cut for BIBO and alternative grating periods in MgO:sPPLT. With the reduction in signal spectral bandwidth using intracavity dispersion control and bandwidth reduction techniques, as well as increase in effective interaction length using larger radius of curvature for mirrors, M_3 and M_4, further increase in UV power is expected. The obtained results show the viability of the demonstrated approach for generation of high-repetition-rate picosecond pulses with extended tunability and practical average powers in the UV.

Funding. Ministry of Economy and Competitiveness (MINECO), Spain (nuOPO, TEC2015-68234-R), Generalitat de Catalunya (ACCIÓ, project VALTEC13-1-0003; AGAUR, project SGR 2014-2016), Severo Ochoa Excellence Grant (SEV-2015-0522), and Fundació Privada Cellex.

References

1. K. Sugioka and Y. Cheng, Light: Science & Applications **3**, 1-12 (2014).
2. E. N. Glezer, M. Milosavljevic, L. Huang, R. J. Finlay, T.-H. Her, J. P. Callan, and E. Mazur, Opt. Lett. **21**, 2023 (1996).
3. A. K. Jayasinghe, J. Rohner, and M. S. Hutson, Biomed. Opt. Express **2**, 2590 (2011).
4. A. Sato, S. Kono, K. Saito, K. Sato, and H. Yokoyama, Opt. Express **18**, 2522 (2010).
5. S. Chaitanya Kumar, E. Sanchez Bautista, and M. Ebrahim-Zadeh, Opt. Lett. **40**, 403 (2015).
6. S. Chaitanya Kumar, J. Canals Casals, E. Sanchez Bautista, K. Devi, and M. Ebrahim-Zadeh, Opt. Lett. **40**, 2397 (2015).
7. M. Ghotbi and M. Ebrahim-Zadeh, Opt. Lett. **30**, 3395 (2005).
8. C. Hoyt, M. Sheik-Bahae, and M. Ebrahim-Zadeh, Opt. Lett. **27**, 1543 (2002).
9. S. Chaitanya Kumar, O. Kimmelma, and M. Ebrahim-Zadeh, Opt. Lett. **37**, 1577 (2012).
10. K. Devi, S. Chaitanya Kumar, and M. Ebrahim-Zadeh, Opt. Lett. **37**, 5049 (2012).
11. M. Ghotbi, A. Esteban-Martin, and M. Ebrahim-Zadeh, Opt. Lett. **33**, 345 (2008).
12. C. Gu, M. Hu, J. Fan, Y. Song, B. Liu, L. Chai, C. Wang, and D. T. Reid, Opt. Express **23**, 6181 (2015).
13. S. Chaitanya Kumar and M. Ebrahim-Zadeh, Opt. Lett. **38**, 5349 (2013).
14. G. K. Samanta, S. Chaitanya Kumar, A. Aadhi, and M. Ebrahim-Zadeh, Opt. Express **22**, 11476 (2014).
15. K. Devi, S. Chaitanya Kumar, and M. Ebrahim-Zadeh, Opt. Express **21**, 24829 (2013).
16. H. Hellwig, J. Liebertz, and L. Bohaty, J. Appl. Phys. **88**, 240 (2000).

References with title

1. K. Sugioka and Y. Cheng, "Ultrafast lasers-reliable tools for advanced materials processing," Light: Science & Applications **3**, 1-12 (2014).
2. E. N. Glezer, M. Milosavljevic, L. Huang, R. J. Finlay, T.-H. Her, J. P. Callan, and E. Mazur, "Three dimensional optical storage inside transparent materials," Opt. Lett. **21**, 2023-2025 (1996).
3. A. K. Jayasinghe, J. Rohner, and M. S. Hutson, "Holographic UV laser microsurgery," Biomed. Opt. Express **2**, 2590-2599 (2011).
4. A. Sato, S. Kono, K. Saito, K. Sato, and H. Yokoyama, "A high-peak-power UV picosecond-pulse light source based on a gain-switched 1.55 micron laser diode and its application to time-resolved spectroscopy of blue violet materials," Opt. Express **18**, 2522-2527 (2010).
5. S. Chaitanya Kumar, E. Sanchez Bautista, and M. Ebrahim-Zadeh, "Stable, high-power, Yb-fiber-based, picosecond ultraviolet generation at 355 nm using BiB_3O_6,"Opt. Lett. **40**, 403-406 (2015).
6. S. Chaitanya Kumar, J. Canals Casals, E. Sanchez Bautista, K. Devi, and M. Ebrahim-Zadeh, "Yb-fiber-laser-based, 1.8 W average power, picosecond ultraviolet source at 266 nm," Opt. Lett. **40**, 2397-2400 (2015).
7. M. Ghotbi and M. Ebrahim-Zadeh, "990 mW average power, 52% efficient, high-repetition-rate picosecond pulse generation in the blue with BiB_3O_6," Opt. Lett. **30**, 3395-3397 (2005).
8. C. Hoyt, M. Sheik-Bahae, and M. Ebrahim-Zadeh, "High-power picosecond optical parametric oscillator based on periodically poled lithium niobate," Opt. Lett. **27**, 1543-1545 (2002).
9. S. Chaitanya Kumar, O. Kimmelma, and M. Ebrahim-Zadeh, "High-power, Yb-fiber-laser-pumped, picosecond parametric source tunable across 752-860 nm," Opt. Lett. **37**, 1577-1579 (2012).
10. K. Devi, S. Chaitanya Kumar, and M. Ebrahim-Zadeh, "High-power, continuous-wave, single-frequency, all-periodically-poled, near-infrared source," Opt. Lett. **37**, 5049-5051 (2012).
11. M. Ghotbi, A. Esteban-Martin, and M. Ebrahim-Zadeh, "Tunable, high-repetition-rate, femtosecond pulse generation in the ultraviolet," Opt. Lett. **33**, 345-347 (2008).
12. C. Gu, M. Hu, J. Fan, Y. Song, B. Liu, L. Chai, C. Wang, and D. T. Reid, "High power tunable femtosecond ultraviolet laser source based on an Yb-fiber-laser pumped optical parametric oscillator," Opt. Express **23**, 6181-6186 (2015).
13. S. Chaitanya Kumar and M. Ebrahim-Zadeh, "Fiber-laser-based green-pumped picosecond MgO:sPPLT optical parametric oscillator,"Opt. Lett. **38**, 5349-5352 (2013).
14. G. K. Samanta, S. Chaitanya Kumar, A. Aadhi, and M. Ebrahim-Zadeh, "Yb-fiber-laser-pumped, high-repetition-rate picosecond optical parametric oscillator tunable in the ultraviolet," Opt. Express **22**, 11476-11487 (2014).
15. K. Devi, S. Chaitanya Kumar, and M. Ebrahim-Zadeh, "Tunable, continuous-wave, ultraviolet source based on intracavity sum-frequency-generation in an optical parametric oscillator using BiB_3O_6," Opt. Express **21**, 24829-24836 (2013).
16. H. Hellwig, J. Liebertz, and L. Bohaty, "Linear optical properties of the monoclinic bismuth borate BiB_3O_6," J. Appl. Phys. **88**, 240-244 (2000).